

This item is the archived peer-reviewed author-version of:

Photoactive layers for photovoltaics based on near-infrared absorbing aryl-substituted naphthalocyanine complexes : preparation and investigation of properties

Reference:

Dubinina Tatiana, Maklakov Sergey, Petrusevich Elizaveta, Borisova Nataliya E., Trashin Stanislav, De Wael Karolien, Tomilova Larisa G..- Photoactive layers for photovoltaics based on near-infrared absorbing aryl-substituted naphthalocyanine complexes : preparation and investigation of properties
New journal of chemistry - ISSN 1144-0546 - 45:32(2021), p. 14815-14821
Full text (Publisher's DOI): <https://doi.org/10.1039/D1NJ02793J>
To cite this reference: <https://hdl.handle.net/10067/1798840151162165141>



Photoactive layers for photovoltaics based on near-infrared absorbing aryl-substituted naphthalocyanine complexes: preparation and investigation of properties

Received 00th January 20xx,
Accepted 00th January 20xx

DOI: 10.1039/x0xx00000x

www.rsc.org/

Tatiana V. Dubinina,^{a,b} Sergey S. Maklakov,^c Elizaveta F. Petrusevich,^d Nataliya E. Borisova,^{a,e} Stanislav A. Trashin,^{f,g} Karolien De Wael,^{f,g} Larisa G. Tomilova^{a,b}†

Photoactive layers based on aryl- and aryloxy-substituted naphthalocyanines and conductive polymer poly[2-methoxy-5-(2'-ethylhexyloxy)-1,4-phenylene vinylene] (MEH-PPV) were prepared using the spin-coating technique and their conductivity was tested in dark and under illumination. For this purpose novel octa-2-naphthoxy-substituted naphthalocyanines were synthesized starting from 6,7-di(2-naphthoxy)naphthalene-2,3-dicarbonitrile. For those novel naphthalocyanine complexes, spectral and electrochemical data were measured and compared with corresponding ones for other aryl-substituted analogues. In comparison to the previously studied naphthalocyanines with alkyl- and phenyl-groups, the formal oxidation and reduction potentials were rather similar. All target complexes demonstrate intense near-infrared absorption at 760-790 nm, which is about 30 nm bathochromically shifted in thin films. The photo-resistive effect was found increasing from composites comprised of naphthoxy- to phenyl-substituted naphthalocyanines. This peculiarity was explained by using optical and atomic force microscopy in terms of different sizes of aggregates formed. The photo-response time for novel composites was approximately 3 s, which is about 20 times faster than measured previously for the films deposited via the drop-casting technique.

Introduction

A significant part of the solar radiation spectrum lies in the near-IR region (740-1400 nm). Thus, the synthesis of near-IR-absorbing compounds with useful photochemistry is an important challenge in the creation of solar cells and light-driven energy conversion. Thanks to high thermal and photochemical stability, high extinction coefficients ($\lg \epsilon \geq 5$),

semi-conductive properties and many possibilities for structural modifications, phthalocyanines and their analogues find applications as electron donors or acceptors in solar cells.¹⁻⁴ There are several groups of near-IR-absorbing phthalocyanines and their analogues such as phthalocyanines with an extended π -system (naphthalocyanines, planar polynuclear phthalocyanines),⁵⁻¹⁰ 3,6-substituted phthalocyanines¹¹⁻¹⁴ and double decker complexes.¹⁵⁻²⁰ Linear annulations of the phthalocyanine core going from phthalocyanines to 2,3-naphthalocyanines lead to a bathochromic shift of about 100 nm in the main absorption maximum (so called "100 nm" rule^{7, 21}). Further benzoannulation going from 2,3-naphthalocyanines to antracocyanines results in the loss of stability of the target compounds towards oxidation. This happens because the first oxidation potentials for antracocyanines shift to near zero volt.^{8, 22} In contrast to double-decker complexes, the absorption in the near-IR region for 2,3-naphthalocyanines is more intense. This results from the nature of corresponding electronic transitions. The red valence and intervalence bands in the near IR region of double-decker complexes are assigned to forbidden transitions²³. On the other hand, the near-IR Q band of 2,3-naphthalocyanines is assigned to an allowed transition and thus, becomes the most intense absorption band.

^a Chemistry Department, M.V. Lomonosov Moscow State University, 1 Leninskie Gory, 119991 Moscow, Russian Federation. E-mail: dubinina.t.vid@gmail.com

^b Institute of Physiologically Active Compounds, Russian Academy of Sciences, 1 Severny proezd, 142432 Chernogolovka, Moscow Region, Russian Federation

^c Institute for Theoretical and Applied Electromagnetics, Russian Academy of Sciences, 125412, 13 Izhorskaya St., Moscow, Russian Federation

^d Theoretical Photochemistry and Photophysics Group, Faculty of Chemistry, Wrocław University of Science and Technology, Wyb. Wyspiańskiego 27, Wrocław PL-50370, Poland

^e N.A. Nesmeyanov Institute of Organoelement Compounds, 28 Vavilov Str. 119334 Moscow, Russian Federation

^f AXES research group, Groenenborgerlaan 171, University of Antwerp, 2020 Antwerp, Belgium

^g Nanolab Center of Excellence, Groenenborgerlaan 171, University of Antwerp, 2020 Antwerp, Belgium

† Authors are mourning the loss of Larisa Tomilova, who suddenly and unexpectedly passed away on the 4 of January 2021. The memory of her will forever remain in the hearts of all friends, colleagues, and students who knew and respected her.

Electronic Supplementary Information (ESI) available: [details of any supplementary information available should be included here]. See DOI: 10.1039/x0xx00000x

However, the synthetic strategies to planar polynuclear phthalocyanines^{5, 24-27} and low symmetry derivatives^{28, 29} are more complicated and result in low yields (typically 10-20%) compared procedures for preparation of 2,3-naphthalocyanines. From this view, 2,3-naphthalocyanines are more advantageous comparing to other near-IR absorbing analogues. Moreover, introduction of peripheral substituents may further tune their optical, photochemical and electrochemical properties. In particular, the introduction of aromatic groups results in increased intermolecular π - π interactions and a better conductivity of thin-film materials.^{17, 30}

Aryloxy-substituted phthalocyanines and naphthalocyanines show a higher solubility comparing to aryl-substituted derivatives and can be comparatively easily prepared.^{18, 31} Thus, 2-naphthoxy-groups were chosen in this work as the peripheral substituents to prepare and characterize the novel π -extended 2-naphthoxy-substituted naphthalocyanines.

Experimental

Materials and methods

Column chromatography was carried out on neutral MN-Aluminium oxide. Preparative TLC was performed using Merck Aluminium Oxide F₂₅₄ neutral flexible plates. All reactions were TLC and UV/Vis controlled until complete disappearance of the starting reagents if not additionally specified. Electronic absorption (UV/Vis) spectra were recorded on a ThermoSpectronic Helios- α spectrophotometer using quartz cells (1×1cm). Matrix assisted laser desorption/ionization time-of-flight (MALDI TOF) mass spectra were taken on a Bruker Ultraflex II mass spectrometer with 2,5-dihydroxybenzoic acid (DHB) as the matrix. High-resolution MALDI mass spectra were registered on a Bruker ULTRAFLEX II TOF/TOF instrument with DHB as the matrix.

¹H and ¹³C NMR spectra were recorded on a Bruker AVANCE 400 spectrometer (400.13 and 100.61 MHz). ¹H-¹H NOESY spectra were registered on a Bruker AVANCE 600 spectrometer (600.13 MHz for ¹H and 150.90 MHz for ¹³C) at room temperature. Chemical shifts are given in ppm relative to SiMe₄.

FTIR spectra were measured using IR 200 Thermo Nicolet spectrometer. Spectral resolution: $\Delta\lambda = 4 \text{ cm}^{-1}$.

The salts Zn(OAc)₂×2H₂O and Mg(OAc)₂×4H₂O were dried immediately before use for 4 h at 70°C.

Electrochemical properties were studied using Autolab PGSTAT302N (Metrohm Autolab B.V.) and a conventional three-electrode cell equipped with Pt-disk working (2.0 mm in diameter) and Pt-rod counter electrodes. *o*-Dichlorobenzene (*o*-DCB, 99%, J&K) containing 0.1 M TBABF₄ (Sigma-Aldrich) was used as supporting electrolyte. The working electrode was refreshed by polishing on an abrasive paper (P800), sonicated in ultrapure water and dried with a heat gun. A double junction Ag/AgCl reference electrode (Metrohm 6.0726.100) was used as the reference electrode. Ferrocene was taken as the internal reference to align the potential scale. All measurements were conducted under nitrogen.

Photoconductive thin films were deposited with a spin-coating technique. First, 4 mg of each dye was mixed with 2 mg of the MEH-PPV

(Poly[2-methoxy-5-(2-ethylhexyloxy)-1,4-phenylenevinylene], average M_n 40000-70000, Aldrich 541443) in 0.25 ml of toluene. The mixtures were kept for 30 min in an ultrasonic bath. Thin films were deposited onto interdigital electrodes made of platinum. The substrate was poly-Al₂O₃, the leakage current was lower than 8×10⁻¹¹. The distance between electrodes was 100 μm . The spin-coating program consisted of two steps: 10 s at 500 rpm and then 50 s at 2500 rpm. Immediately after the deposition, these films were kept at a fore-vacuum for 24 hrs to remove the solvent and decrease interaction with air. Current-voltage dependencies were measured from -5 to +5 V at a 50 mV/s sweep rate. The illuminance with the tungsten light was 40 kLx. Time-dependencies were measured in a potentiostatic mode at 1 V. The tungsten light was chosen to mimic sunlight and decrease electric noise. The Solartron electrochemical interface 1287 was used for the measurements.

Preparation of 6,7-di(2-naphthoxy)naphthalene-2,3-dicarbonitrile 2:

A mixture of 6,7-dibromonaphthalene-2,3-dicarbonitrile **1** (1.37 g, 4.0 mmol), β -naphthol (2.33 g, 16.2 mmol) and anhydrous K₂CO₃ (5.50 g, 39.9 mmol) were stirred in dry DMF (27 mL) under Ar at 130°C for 7h (TLC-control: Al₂O₃, ethyl acetate : *n*-hexane (1:10, V:V)). The reaction mixture was cooled to room temperature and water (100 mL) was added. The product was collected by filtration and washed by water up to neutral pH. Then the precipitate was purified by flash chromatography (Al₂O₃, toluene). The fractions, which were moved by ethyl acetate and were additionally recrystallized from *n*-hexane. This yielded compound **2** (1.00 g, 54%). m.p.=215°C (760 mmHg), R_f = 0.40 (Al₂O₃, ethyl acetate : *n*-hexane (1:10, V:V)). ¹H NMR (400.13 MHz, CDCl₃): 7.33 (s, 2H, β H); 7.34-7.36 (m, 2H, H_{ONaph}); 7.52-7.57 (m, 6H, H_{ONaph}); 7.80-7.82 (m, 2H, H_{ONaph}); 7.91-7.93 (m, 2H, H_{ONaph}); 7.95-7.98 (m, 2H, H_{ONaph}); 8.05 (s, 2H, α H). ¹³C NMR (100.61 MHz, CDCl₃): δ 109.14 (C_{quaternary}); 114.40 (C_{tertiary}); 115.92 (CN); 116.55 (C_{tertiary}); 119.97 (C_{tertiary}); 125.81 (C_{tertiary}); 127.03 (C_{tertiary}); 127.41 (C_{tertiary}); 127.95 (C_{tertiary}); 130.31 (C_{quaternary}); 130.67 (C_{tertiary}); 131.16 (C_{quaternary}); 134.08 (C_{tertiary}); 134.21 (C_{quaternary}); 152.36 (C_{quaternary}); 152.52 (C_{quaternary}). MS (EI): m/z 462 [M].

Preparation of 3,4,12,13,21,22,30,31-octa-(2-naphthoxy)-2,3-naphthalocyaninato zinc 3a:

A mixture of 6,7-di(2-naphthoxy)naphthalene-2,3-dicarbonitrile **2** (0.15 g, 0.32 mmol), Zn(OAc)₂×2H₂O (0.030 g, 0.14 mmol), MeOLi (0.012 g, 0.32 mmol) and a few drops of DBU were refluxed in *i*-AmOH (2 mL) for 8 h (UV/Vis and TLC (Al₂O₃, C₆H₆) control). The reaction mixture was cooled to room temperature and a MeOH:H₂O (10:1 V/V) mixture was added. The precipitate was filtered and washed with water and MeOH. This yielded **3a** (0.14 mg, 92%). UV/Vis λ_{max} (THF)/nm 331 (lg ϵ 5.18), 687 (4.68) and 768 (5.40). ¹H NMR δ_{H} (600.13 MHz, [D₅]Py) 7.48-7.56 (24H, m, H_{ONaph}); 7.71-7.74 (8H, m, H_{ONaph}); 7.91-8.06 (24H, m, H_{ONaph}); 8.39 (8H, s, β H) and 9.88 (8H, s, α H). IR (KBr): ν (cm⁻¹) 903-1034 (C-O-C st sym); 1001-1252 (C-O-C st as) and 1493-1628 (ν pyrrole). MS (MALDI-TOF)

m/z 1626 (M-2ONaph, 56%); 1769 (M-ONaph, 100%) and 1912 (M^+ , 56%).

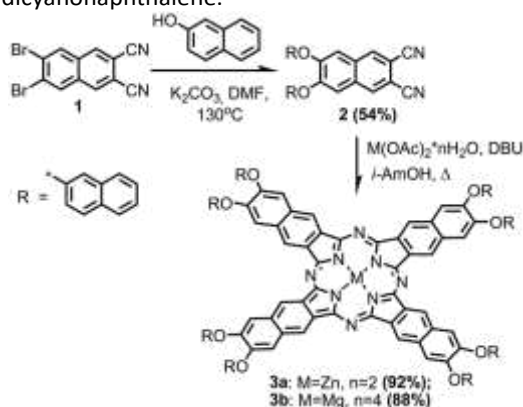
Preparation of 3,4,12,13,21,22,30,31-octa-(2-naphthoxy)-2,3-naphthalocyaninato magnesium 3b:

A mixture of 6,7-di(2-naphthoxy)naphthalene-2,3-dicarbonitrile **2** (0.10 g, 0.22 mmol), $Mg(OAc)_2 \cdot 4H_2O$ (0.023 g, 0.11 mmol), MeOLi (0.082 mg, 0.22 mmol) and a few drops of DBU were refluxed in *i*-AmOH (2 mL) for 7 h (UV/Vis and TLC (Al_2O_3 , C_6H_6) control). The reaction mixture was cooled to room temperature and a MeOH:H₂O (10:1 V/V) mixture was added. The precipitate was filtered and washed with water and MeOH. This yielded **3b** (89 mg, 88%). UV/Vis λ_{max} (THF)/nm 361 (lge 5.02), 681 (4.72) and 766 (5.45). 1H NMR δ_H (600.13 MHz, $[D_5]Py$) 7.48–7.54 (24H, m, H_{ONaph}); 7.71–7.74 (8H, m, H_{ONaph}); 7.88–8.04 (24H, m, H_{ONaph}); 8.42 (8H, s, βH) and 10.01 (8H, s, αH). IR (Vaseline oil): ν (cm^{-1}) 916–1034 (C–O–C st sym); 1034–1255 (C–O–C st as) and 1598–1630 (ν pyrrole). MS (MALDI-TOF) m/z 1586 (M-2ONaph, 34%); 1729 (M-ONaph, 100%) and 1872 (M^+ , 64%).

Results and discussion

Synthesis and Characterization

Naphthalocyanine periphery was functionalized using a nucleophilic substitution reaction at the stage of the preparation of an initial dicyano-naphthalene. 6,7-Dibromo-2,3-dicyanonaphthalene appears to be a convenient synthetic block for the introduction of 2-naphthoxy groups. Nucleophilic substitution reaction took place in strongly anhydrous conditions: dry DMF and freshly calcined K_2CO_3 (Scheme 1). Attempts to use DMF, which contains traces of water, led to increased quantity of oligomerized byproducts. The nucleophilic substitution process is activated by two electron-withdrawing CN groups and does not need any additional catalyst. Target 2,3-dicyanonaphthalene was obtained at a temperature by 40°C higher than used for aryloxy-substituted *o*-phthalonitriles.^{32, 33} It results from an increase in the distance between electron-withdrawing cyano-groups and the center of nucleophilic attack going from *o*-phthalonitrile to 2,3-dicyanonaphthalene.



Scheme 1. Synthesis of target complexes.

Purification of target compound **2** from the naphthalocyanine-like products of oligomerization was made using column chromatography and recrystallization.

Zinc and magnesium complexes were obtained from nitrile **2** using template macrocyclization in a boiling isoamylic alcohol, in a presence of 1,8-diazabicyclo(5.4.0)undec-7-ene (DBU) as a base. Compounds **3a** and **3b** were obtained as dark-greenish powders in high yields. Zn and magnesium were chosen as central ions due to their propensity for demetallation and further metallation by the wide range of metal cations.^{34, 35} Target complexes were identified by MALDI TOF mass spectrometry, NMR and IR spectroscopy.

In the mass spectra of both complexes **3** intense molecular ions were found. Additionally, two fragmentation peaks, which resulted from cleavage of one and two naphthoxy-groups respectively, were observed. Isotopic patterns for molecular ions are in a good agreement with theoretically calculated ones and depend on the nature of central ion.

In FTIR spectra of both complexes **3** skeletal vibrations of the pyrrole fragments occupy the region from 1493 to 1630 cm^{-1} . The bands at 903–1034 cm^{-1} and 1034–1255 cm^{-1} were assigned to symmetrical and asymmetrical stretching vibrations of C–O–C bonds.

In order to reach a finer signal resolution in the 1H NMR spectra of naphthalocyanines **3a** and **3b** polar coordinating solvent $Py-d_5$ was used. The downfield shift of αH protons was observed due to the deshielding effect of the porphyrazine core. The assignment of signals in 1H NMR spectra was made using 2D NOESY NMR spectroscopy. Cross peaks were observed between the signals of αH and βH protons and between signals of βH and protons of naphthoxy groups. Additionally group of cross peaks was found between signals of different protons of naphthoxy groups.

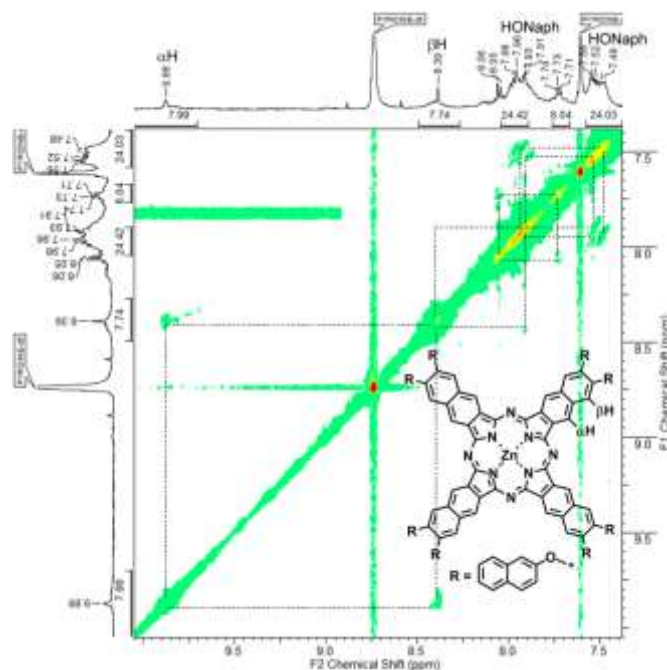


Fig.1. 1H - 1H NOESY NMR for complex **3a** in $[D_5]Py$.

Due to the both bulky and weak electron-withdrawing nature of naphthoxy groups deshielding effect for αH and βH protons was observed for target complexes comparing to octaphenyl-,

octaphenoxy- and octa-(3-(ethylthio)phenyl)substituted 2,3-naphthalocyanine complexes, which were described by us earlier (Table 1). In this row of peripheral substituents, phenyl groups show the strongest electron-donating nature and lowest steric hindrance.

Table 1. ^1H NMR data for complexes **3a**, **3b** and some literature data for comparison.

| Compound | αH | βH | Solvent |
|---------------------------------|------------------|-----------------|--------------------------|
| 3a | 9.88 | 8.39 | $[\text{D}_5]\text{Py}$ |
| 3b | 10.01 | 8.42 | $[\text{D}_5]\text{Py}$ |
| $\text{PhO}^8\text{NcMg}^{18}$ | 9.54 | 8.03 | $[\text{D}_8]\text{THF}$ |
| $\text{EtSP}^8\text{NcZn}^{36}$ | 9.27 | 8.47 | $[\text{D}_8]\text{THF}$ |
| $\text{Ph}^8\text{NcMg}^{35}$ | 8.66 | 8.21 | $[\text{D}_5]\text{Py}$ |

UV/Vis spectra of target complexes were measured in THF solutions and thin films. There are two main absorption maxima: *B* band (350–370 nm) and *Q* band (760–790 nm). As it is usually observed for lanthanide (III), Zn and Mg monophthalocyanines the nature of the central ion does not influence the *Q* band position.^{35, 37–39} Strong intermolecular interactions in a film results in broadening of the *Q* band and a ca 30 nm bathochromic shift of its maximum (Fig.2). A similar effect was recently demonstrated for Langmuir–Schaefer 25-layer films of phenyl-substituted Zn naphthalocyanine.⁴⁰

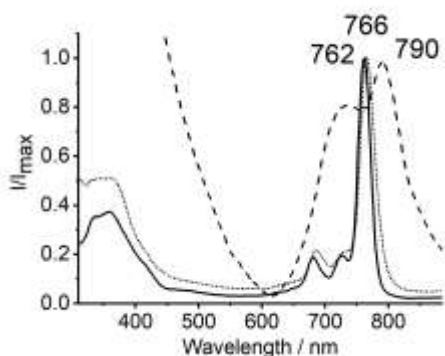


Fig. 2. UV/Vis spectra of compound **3b** in THF (dotted line), in film (dashed line) and PhO^8NcMg in THF (solid line).

In comparison with earlier described phenoxysubstituted 2,3-naphthalocyaninato magnesium,¹⁸ for naphthoxysubstituted an analogue 4 nm bathochromic shift of *Q* band is found. It can be explained by the extension of the aromatic π -system of peripheral groups going from phenoxy- to naphthoxy-substituted complexes.

The redox properties of **3a** and **3b** were studied on a Pt disk electrode using cyclic voltammetry (CV) and square wave voltammetry (SWV). Two oxidation and two reduction transitions were clearly observed (Figure 3, Table 2). In the region of Red_2 , the magnesium complex (**3b**) gave two peaks, which can be a result of a split due to aggregation. The intensity of the second peak (at -2.13 V) was sensitive to the scan rate and equilibration duration for the fresh working

electrode in the solution. This indicates about the contribution of adsorption in this peak. Since some broadening in peaks was also observed for Ox_1 and Ox_2 , the additional peak at Red_2 was attributed to complications due to aggregation and adsorption but not an additional redox transition in **3b**. Moreover, this additional peak was not observed in **3a**.

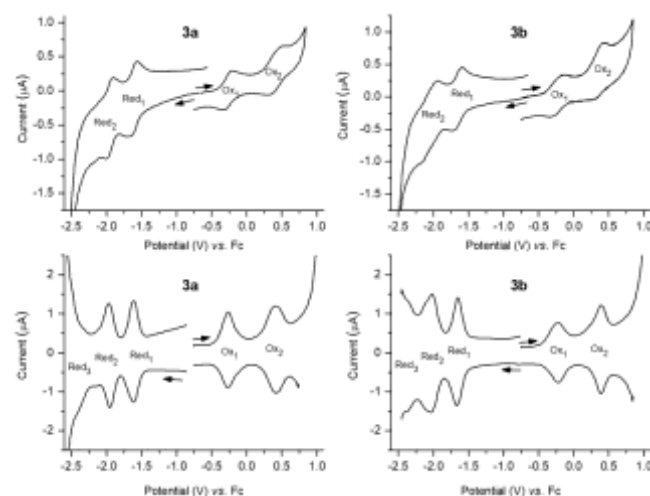


Fig. 3. CV (top) and SWV (bottom) of the target complexes **3a** and **3b** in *o*-DCB containing 0.1 M TBABF₄ as the supporting electrolyte. Scan rate, 0.1 V/s. SW amplitude, 0.05 V. SW frequency, 10 Hz.

Noteworthy, the second oxidation Ox_2 was reversible, which is the feature of naphthalocyanines in contrast to phthalocyanines. At potentials higher than Ox_2 , electrode passivation occurred, which could be reversed by short stirring of the solutions. This passivation likely originates from strong aggregation and even oligomerization of the oxidized forms. Moreover, the current steeply rises at potentials above +0.9 V but an irreversible oxidation peak Ox_3 was not observed at least till +1.1 V, possibly due to also steeply rising background hindering the peak. The irreversible oxidation Ox_3 is expected at these potentials since Ox_3 was observed at +0.93 V for a similar naphthalocyanine Ph^8NcMg ²⁷. In comparison to the previously studied naphthalocyanines with electron-donating substituents, the formal oxidation and reduction potentials were rather similar. The average first oxidation and reduction potential were at -0.26 ± 0.02 and -1.63 ± 0.03 V, respectively (Table 2).

Table 2. Formal reduction and oxidation potentials (E°) vs Fc^{+/0} in *o*-DCB.

| | Reduction | | | Oxidation | |
|--|----------------|----------------|----------------|---------------|---------------|
| | Red_3 | Red_2 | Red_1 | Ox_1 | Ox_2 |
| NaphthO ⁸ NcZn (3a) | $-2.41^{[a]}$ | -1.96 | -1.61 | -0.27 | $+0.42$ |
| NaphthO ⁸ NcMg (3b) | $-2.35^{[a]}$ | $-2.02; -2.13$ | -1.65 | -0.24 | $+0.38$ |
| 2-Np ⁸ NcZn ⁴¹ | -2.15 | -1.97 | -1.63 | -0.23 | $+0.53$ |
| $\text{Ph}^8\text{NcMg}^{27}$ | -2.31 | -1.99 | -1.62 | -0.29 | $+0.45^{[b]}$ |
| <i>t</i> -Bu ⁴ NcZn ⁴² | - | - | -1.66 | -0.29 | - |

^[a] approximate potential; ^[b] an additional transition Ox_3 at +0.93 V.

Photoconductive thin films were deposited with a spin-coating technique. Both composites comprised of the MEH-PPV matrix and Ph^8NcMg or $\text{NaphthO}^{\text{NcZn}}$ (**3a**) dye were conductive and increased conductivity under illumination. HOMO and LUMO levels of naphthoxy- and phenyl- substituted zinc complexes were calculated using electrochemical data:

$$E_{\text{HOMO}} = -1.4 \times E_{\text{Ox}} - 4.6$$

$$E_{\text{LUMO}} = -4.8 - E_{\text{Red}}$$

E_{HOMO} and E_{LUMO} values obtained for both complexes from this equation^{43, 44} equal to -4.2 eV and -3.2 eV respectively. Whereas the LUMO level is close in value to the LUMO level of MEH-PPV ($E_{\text{LUMO}} = -3.0$ eV), the HOMO level of MEH-PPV lies lower in energy scale ($E_{\text{HOMO}} = -5.3$ eV). Thus, target naphthalocyanines can be an electron donor for blend binary devices comprising from naphthalocyanines and MEH-PPV.

The photo-resistive effect differed in quantity with the dye. Taking into account the film thickness of approximately 100 nm, the conductivity σ of the $\text{NaphthO}^{\text{NcZn}}$ -based composite was 2.1×10^{-9} S/cm (resistivity was 4.9×10^8 Ohm-cm) and 3.6×10^{-11} S/cm (2.8×10^{10} Ohm-cm) was conductivity of the Ph^8NcMg -based layer. The photo-resistive effect, $\sigma_{\text{light}}/\sigma_{\text{dark}}$, was 2 and 200, respectively (see Fig. 4 and Fig. 5). Two factors might influence the conductivity and the photo-resistive effect: the microstructure of the composite and the difference in photoelectric activity of the dye. Since the difference in the UV-VIS absorption spectra of the dyes was insignificant, the latter was negligible.

The difference in microstructure of the two composites studied was in the homogeneity of the layers. Dark dots that can be seen in Fig. 6 of approximately 1-10 μm are micro-particles of the dyes. This value was lower than that usually observed for aggregates of particles of phthalocyanines¹⁷ and showed good intermixture provided by ultrasonic treatment.

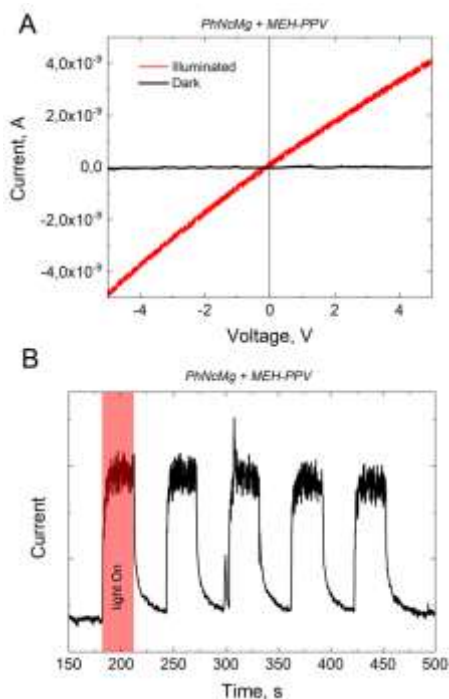


Fig. 4. Current-voltage (A) and current-time (B) dependencies measured from the " Ph^8NcMg + MEH-PPV" composite layer.

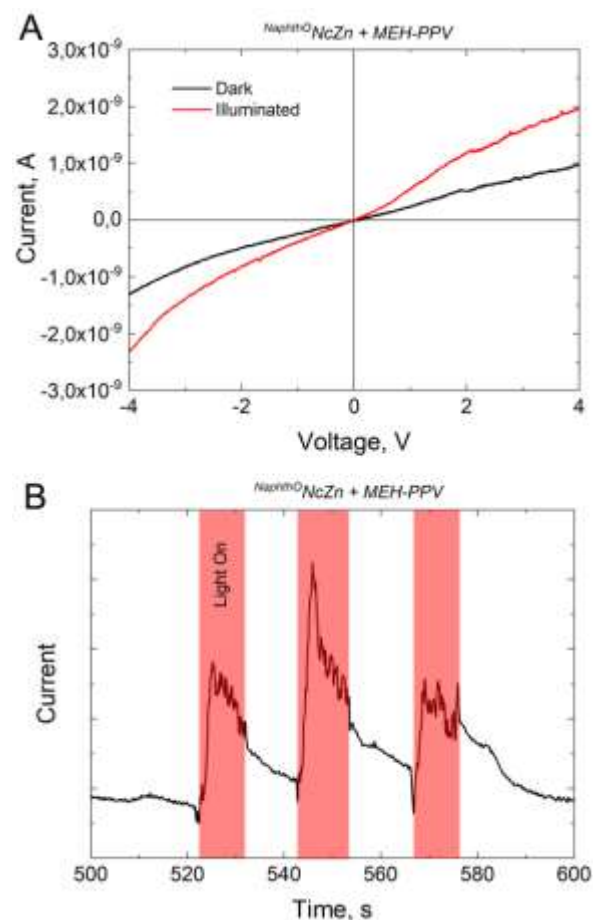


Fig. 5. Current-voltage (A) and current-time (B) dependencies measured from the " $\text{NaphthO}^{\text{NcZn}}$ + MEH-PPV" composite layer.

Boundaries between $\text{NaphthO}^{\text{NcZn}}$ (**3a**) and MEH-PPV were blurred and the composite was quite homogeneous (Fig. 6B). This resulted in higher conductivity but gave a low photo-resistive effect.

The Ph^8NcMg particles were distinctly separated from the MEH-PPV matrix (Fig. 6A). Both micro- and macro-inhomogeneity (Fig. 6A) of this composite resulted in lower conductivity but proved to give a good photo-resistive effect. This was following the known typical value for the length of the interface in multi-component organic semiconductors that serves effectively for charge carriers separation and is of ~ 30 nm.⁴⁵ The response time was approximately 3 s for both composites. This was significantly faster than measured previously from the films deposited *via* a drop-casting technique.⁴⁵

It can be noted, that the value of extinction coefficient, measured for $\text{NaphthO}^{\text{NcZn}}$ is higher than for Ph^8NcMg (Fig.S9 and Fig.S10). So the presence of bulky naphthoxy-groups in naphthalocyanine macrocycle suppresses the aggregation and respectively increases charge generation for $\text{NaphthO}^{\text{NcZn}}$ relative to Ph^8NcMg . This phenomenon additionally supports the higher conductivity of $\text{NaphthO}^{\text{NcZn}}$.

There are no conflicts to declare.

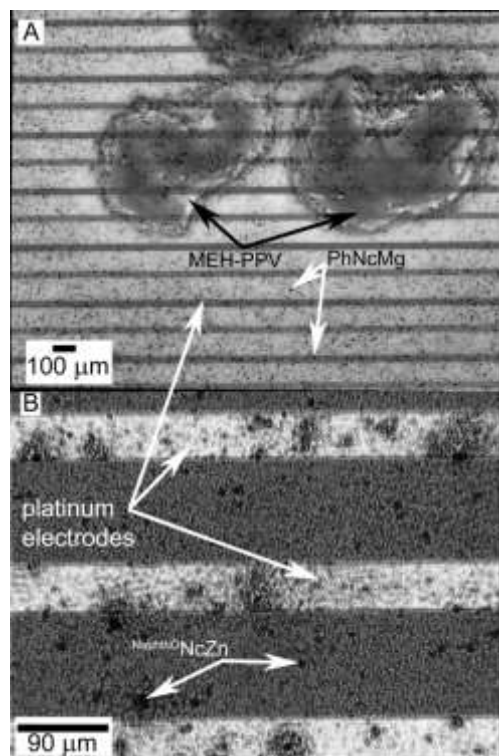


Fig. 6. Optical microscopy images of the “Ph⁸NcMg + MEH-PPV” (A) and “NaphthO NcZn + MEH-PPV” (B) composite layers deposited onto interdigital platinum electrodes.

Conclusions

Photoactive layers comprised of aryl-substituted (phenyl- and 2-naphthoxy-) naphthalocyanines in polymer matrix were obtained. It has emerged that spin-coating technique allows to obtain more homogeneous thin films with about a 20 times faster photoresponse compared to drop casted films. Due to the aggregation, which was proven by microscopy data, the photoresistive effect, $\sigma_{\text{light}}/\sigma_{\text{dark}}$ of phenyl-substituted complex is higher than for the naphthoxy-substituted analogue.

Electrochemical measurements showed that naphthoxy-substituted complexes have the same first oxidation and reduction potentials as described for phenyl-substituted complexes.

The extension of the π -system of aromatic substituents on the periphery of the naphthalocyanine macrocycle results in a small bathochromic shift of the corresponding Q band maximum in UV/Vis spectra of (2-naphthoxy)substituted naphthalocyanines comparing to phenoxy-substituted 2,3-naphthalocyanines. In contrast to spectra in solution, the appearance of strong intermolecular interactions in a film results in a ca. 30 nm bathochromic shift of the absorption maxima of target compounds.

Conflicts of interest

Acknowledgements

Synthesis and identification of target compounds was supported by the Russian Science Foundation Grant № 19-73-00099. Electrochemical measurements were supported by ERA.Net RUS Plus Plasmon Electrolight and FWO funding (RFBR №18-53-76006 ERA).

Notes and references

1. J. Fernández-Ariza, M. Urbani, M. Grätzel, M. S. Rodríguez-Morgade, M. K. Nazeeruddin and T. Torres, *ChemPhotoChem*, 2017, **1**, 164-166.
2. F. Chindeka, P. Mashazi, J. Britton, D. O. Oluwole, S. Mapukata and T. Nyokong, *Journal of Photochemistry and Photobiology A: Chemistry*, 2020, **399**, 112612.
3. T. M. Grant, D. S. Josey, K. L. Sampson, T. Mudigonda, T. P. Bender and B. H. Lessard, *The Chemical Record*, 2019, **19**, 1093-1112.
4. M. G. Walter, A. B. Rudine and C. C. Wamser, *Journal of Porphyrins and Phthalocyanines*, 2010, **14**, 759-792.
5. T. V. Dubinina, N. E. Borisova, K. V. Paramonova and L. G. Tomilova, *Mendeleev Communications*, 2011, **21**, 165-167.
6. A. Muranaka, M. Yonehara and M. Uchiyama, *Journal of the American Chemical Society*, 2010, **132**, 7844-7845.
7. W. Freyer and L. q. Minh, *Monatshefte für Chemie / Chemical Monthly*, 1986, **117**, 475-489.
8. N. Kobayashi, S.-i. Nakajima, H. Ogata and T. Fukuda, *Chemistry – A European Journal*, 2004, **10**, 6294-6312.
9. T. V. Dubinina, L. G. Tomilova and N. S. Zefirov, *Russian Chemical Reviews*, 2013, **82**, 865.
10. S. A. Trashin, T. V. Dubinina, A. V. Fionov and L. G. Tomilova, *Journal of Porphyrins and Phthalocyanines*, 2011, **15**, 1195-1201.
11. N. Kobayashi, H. Ogata, N. Nonaka and E. A. Luk'yanets, *Chemistry – A European Journal*, 2003, **9**, 5123-5134.
12. T. Fukuda, T. Ishiguro and N. Kobayashi, *Tetrahedron Letters*, 2005, **46**, 2907-2909.
13. N. Kobayashi, T. Furuyama and K. Satoh, *Journal of the American Chemical Society*, 2011, **133**, 19642-19645.
14. R. Wang, Y. Zhao, C. Zhu and X. Huang, *Journal of Heterocyclic Chemistry*, 2015, **52**, 1230-1233.
15. V. E. Pushkarev, L. G. Tomilova and V. N. Nemykin, *Coordination Chemistry Reviews*, 2016, **319**, 110-179.
16. J. Jiang, W. Liu, K.-W. Poon, D. Du, D. P. Arnold and D. K. P. Ng, *European Journal of Inorganic Chemistry*, 2000, **2000**, 205-209.
17. T. V. Dubinina, A. D. Kosov, E. F. Petrusevich, S. S. Maklakov, N. E. Borisova, L. G. Tomilova and N. S. Zefirov, *Dalton Transactions*, 2015, **44**, 7973-7981.
18. T. V. Dubinina, R. A. Piskovoi, A. Y. Tolbin, V. E. Pushkarev, M. Y. Vagin, L. G. Tomilova and N. S. Zefirov, *Russian Chemical Bulletin*, 2008, **57**, 1912-1919.

19. W. Zheng, B.-B. Wang, J.-C. Lai, C.-Z. Wan, X.-R. Lu, C.-H. Li and X.-Z. You, *Journal of Materials Chemistry C*, 2015, **3**, 3072-3080.
20. T. V. Dubinina, V. E. Pushkarev, S. A. Trashin, K. V. Paramonova and L. G. Tomilova, *Macroheterocycles*, 2012, **5**, 366-370.
21. E. A. Lukyanets and V. N. Nemykin, *Journal of Porphyrins and Phthalocyanines*, 2010, **14**, 1-40.
22. W. Freyer and S. Flatau, *Tetrahedron Letters*, 1996, **37**, 5083-5086.
23. C. L. Dunford, B. E. Williamson and E. Krausz, *The Journal of Physical Chemistry A*, 2000, **104**, 3537-3543.
24. D. Lelievre, O. Damette and J. Simon, *Journal of the Chemical Society, Chemical Communications*, 1993, 939-940.
25. A. Y. Tolbin, L. G. Tomilova and N. S. Zefirov, *Russian Chemical Reviews*, 2008, **77**, 435-449.
26. S. G. Makarov, O. N. Suvorova and D. Wöhrle, *Journal of Porphyrins and Phthalocyanines*, 2011, **15**, 791-808.
27. T. V. Dubinina, S. A. Trashin, N. E. Borisova, I. A. Boginskaya, L. G. Tomilova and N. S. Zefirov, *Dyes and Pigments*, 2012, **93**, 1471-1480.
28. N. Kobayashi, R. Kondo, S. Nakajima and T. Osa, *Journal of the American Chemical Society*, 1990, **112**, 9640-9641.
29. A. N. Cammidge, V. H. M. Goddard, G. Will, D. P. Arnold and M. J. Cook, *Tetrahedron Letters*, 2009, **50**, 3013-3016.
30. T. V. Dubinina, M. S. Belousov, S. S. Maklakov, V. I. Chernichkin, M. V. Sedova, V. A. Tafeenko, N. E. Borisova and L. G. Tomilova, *Dyes and Pigments*, 2019, **170**, 107655.
31. S. Makarov, C. Litwinski, E. A. Ermilov, O. Suvorova, B. Röder and D. Wöhrle, *Chemistry – A European Journal*, 2006, **12**, 1468-1474.
32. M. J. Plater, A. Jeremiah and G. Bourhill, *Journal of the Chemical Society, Perkin Transactions 1*, 2002, 91-96.
33. E. F. A. Carvalho, M. J. F. Calvete, A. C. Tomé and J. A. S. Cavaleiro, *Tetrahedron Letters*, 2009, **50**, 6882-6885.
34. J. Alzeer, P. J. C. Roth and N. W. Luedtke, *Chemical Communications*, 2009, 1970-1971.
35. T. V. Dubinina, K. V. Paramonova, S. A. Trashin, N. E. Borisova, L. G. Tomilova and N. S. Zefirov, *Dalton Transactions*, 2014, **43**, 2799-2809.
36. T. V. Dubinina, P. I. Tychinsky, N. E. Borisova, S. S. Maklakov, M. V. Sedova, A. D. Kosov, L. G. Tomilova and N. S. Zefirov, *Dyes and Pigments*, 2017, **144**, 41-47.
37. E. A. Kuzmina, T. V. Dubinina, A. V. Zasedatelev, A. V. Baranikov, M. I. Makedonskaya, T. B. Egorova and L. G. Tomilova, *Polyhedron*, 2017, **135**, 41-48.
38. T. V. Dubinina, P. I. Tychinsky, N. E. Borisova, V. I. Krasovskii, A. S. Ivanov, S. V. Savilov, S. S. Maklakov, M. V. Sedova and L. G. Tomilova, *Dyes and Pigments*, 2018, **156**, 386-394.
39. A. D. Kosov, T. V. Dubinina, M. Y. Seliverstov, L. G. Tomilova and N. S. Zefirov, *Macroheterocycles*, 2016, **9**, 201-205.
40. A. V. Kazak, M. A. Marchenkova, T. V. Dubinina, A. I. Smirnova, L. G. Tomilova, A. V. Rogachev, D. N. Chausov, A. A. Stsiapanau and N. V. Usol'tseva, *New Journal of Chemistry*, 2020, **44**, 3833-3837.
41. T. V. Dubinina, E. O. Moiseeva, D. A. Astvatsaturov, N. E. Borisova, P. A. Tarakanov, S. A. Trashin, K. De Wael and L. G. Tomilova, *New Journal of Chemistry*, 2020, **44**, 7849-7857.
42. R. Chitta, A. S. D. Sandanayaka, A. L. Schumacher, L. D'Souza, Y. Araki, O. Ito and F. D'Souza, *The Journal of Physical Chemistry C*, 2007, **111**, 6947-6955.
43. P. I. Djurovich, E. I. Mayo, S. R. Forrest and M. E. Thompson, *Organic Electronics*, 2009, **10**, 515-520.
44. B. W. D'Andrade, S. Datta, S. R. Forrest, P. Djurovich, E. Polikarpov and M. E. Thompson, *Organic Electronics*, 2005, **6**, 11-20.
45. S. S. Maklakov, T. V. Dubinina, M. M. Osipova, E. F. Petrusevich, A. D. Mishin and L. G. Tomilova, *Journal of Porphyrins and Phthalocyanines*, 2016, **20**, 1134-1141.